



Tetraphenylethene-Modified Colorimetric and Fluorescent Chemosensor for Hg²⁺ With Aggregation-Induced Emission Enhancement, Solvatochromic, and Mechanochromic Fluorescence Features

Jin-jin Tian^{1†}, Dian-dian Deng^{1†}, Long Wang¹, Zhao Chen^{1*} and Shouzhi Pu^{1,2*}

OPEN ACCESS

Edited by:

Tony D. James,
University of Bath, United Kingdom

Reviewed by:

Sebastiano Di Pietro,
University of Pisa, Italy
Xurong Qin,
Southwest University, China

*Correspondence:

Zhao Chen
chenzhao666@126.com
Shouzhi Pu
pushouzhi@tsinghua.org.cn

[†]These authors have contributed
equally to this work

Specialty section:

This article was submitted to
Organic Chemistry,
a section of the journal
Frontiers in Chemistry

Received: 08 November 2021

Accepted: 06 December 2021

Published: 26 January 2022

Citation:

Tian J-j, Deng D-d, Wang L, Chen Z
and Pu S (2022) Tetraphenylethene-
Modified Colorimetric and Fluorescent
Chemosensor for Hg²⁺ With
Aggregation-Induced Emission
Enhancement, Solvatochromic, and
Mechanochromic
Fluorescence Features.
Front. Chem. 9:811294.
doi: 10.3389/fchem.2021.811294

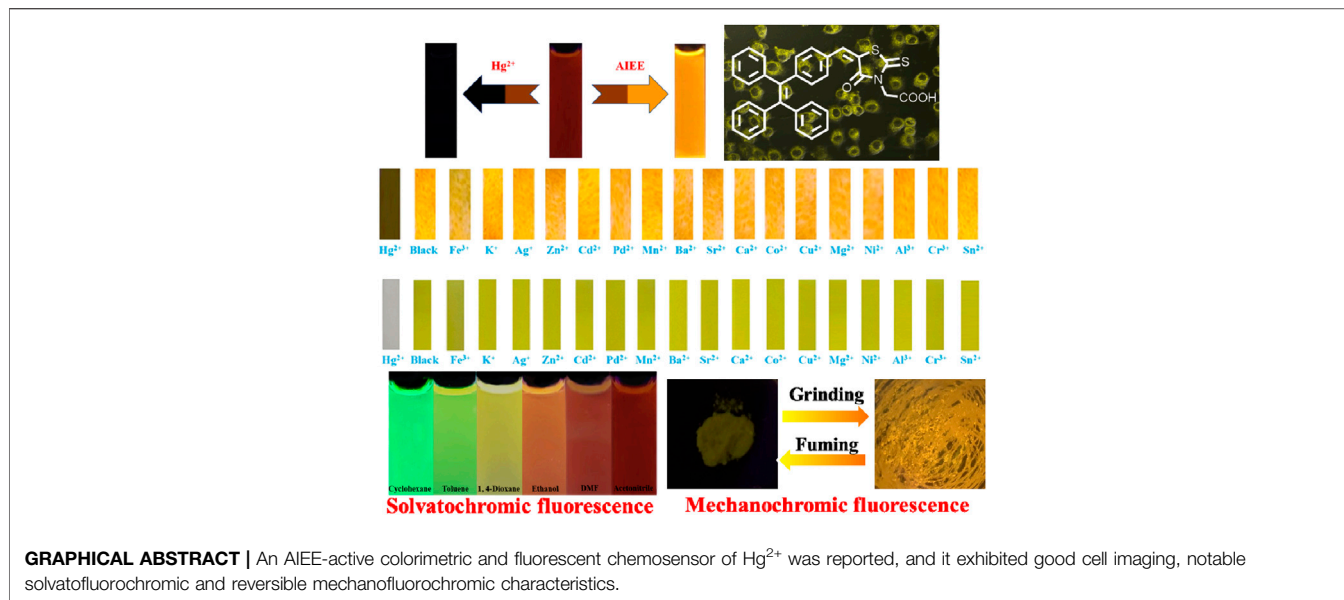
¹Jiangxi Key Laboratory of Organic Chemistry, Jiangxi Science and Technology Normal University, Nanchang, China,
²Department of Ecology and Environment, Yuzhang Normal University, Nanchang, China

A tetraphenylethene (TPE)-modified rhodanine derivative was successfully designed and prepared, and this luminophor showed intramolecular charge transfer nature from the TPE unit to the rhodanine-3-acetic acid unit. Interestingly, this luminogen not only exhibited typical aggregation-induced emission enhancement (AIEE) behavior but also showed good cell imaging performance. Remarkably, this AIEE-active TPE-containing rhodanine derivative possessed noticeable solvatochromic fluorescence effect involving multiple fluorescent colors of green, yellow-green, yellow, orange, and red. Meanwhile, this fluorescogenic compound displayed reversible mechanochromic fluorescence behavior based on the mutual transformation of between stable crystalline and metastable amorphous states. On the other hand, this multifunctional fluorophor could selectively and sensitively detect Hg²⁺ in an acetonitrile solution. Furthermore, this chemosensor could also be used to detect Hg²⁺ on test paper strips.

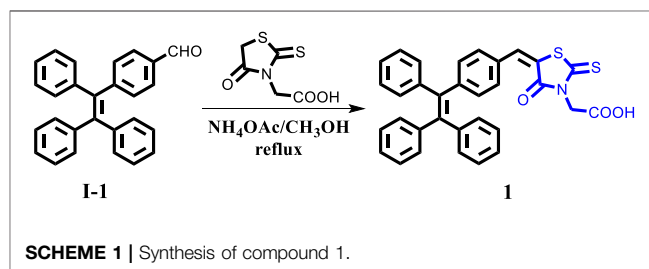
Keywords: rhodanine, chemosensor, aggregation-induced emission enhancement, solvatochromic fluorescence, mechanochromic fluorescence

INTRODUCTION

The exploitation of fluorescent chemosensors for the detection of transition-metal ions has received immense interest because contamination caused by heavy metal ions may have adverse influence on human health and the natural environment (Que et al., 2008; Zhang et al., 2011). Among various transition metal ions, Hg²⁺ is regarded as one of the most dangerous. For example, Hg²⁺ can go through the biofilm and produces serious harm to the central nervous system and endocrine system (Tan et al., 2017; Feng et al., 2017; Gupta et al., 2017; Yang et al., 2018; Li et al., 2018). Indeed, it can induce the formation of many diseases containing kidney failure and cognitive and motion disorder (Bhalla et al., 2010; Yang et al., 2014). Therefore, it is a significant research topic to develop high-efficiency methods for detecting Hg²⁺. Notably, fluorescent sensing has become a powerful tool for the detection of Hg²⁺ (Kiani et al., 2020; Singh et al., 2020; Xu et al., 2020; Tian et al., 2020; Nan et al., 2021). Highly emissive materials in



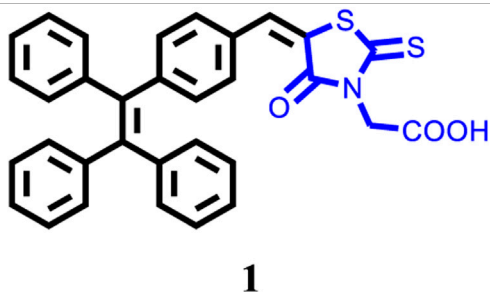
the aggregation state have drawn much attention because of their broad applications in chemical sensing, bioimaging, and photoelectric devices (Tong et al., 2014; Huang et al., 2014; Song et al., 2016; Tang et al., 2019; Zheng et al., 2019; Li et al., 2021; Cheng et al., 2021; Yin et al., 2021; Wang et al., 2021). However, traditional luminogenic molecules commonly suffer from a troublesome luminescence “aggregation-caused quenching (ACQ)” phenomenon (Mei et al., 2015). Fortunately, in 2001, it was discovered by Tang and co-workers that 1-methyl-1,2,3,4,5-pentaphenylsilole showed an interesting “aggregation-induced emission (AIE)” effect, and emitted strong aggregative-state fluorescence (Luo et al., 2001). Subsequently, in 2002, Park et al. reported the “aggregation-induced emission enhancement (AIEE)” effect (An et al., 2002). Obviously, AIE or AIEE phenomenon is opposite to the pernicious ACQ, and AIE or AIEE-active luminophors are more conducive to practical applications. To date, a variety of luminogens possessing AIE or AIEE property have been reported (Dong et al., 2015; Chen et al., 2016; Yang et al., 2016; Ma et al., 2021; Yin et al., 2021). Among them, tetraphenylethene (TPE)-modified fluorescent



molecules have received special attention from researchers due to their excellent aggregative-state emissive performance. When in the aggregates, the structurally twisted TPE molecules cannot pack in through a tight π - π stacking interactions network, and thus restrict the formation of ACQ effect. Meanwhile, the restricted intramolecular rotations block the non-radiative decays and open up the radiative channels.

Solvatochromism is an interesting phenomenon, which involves a color change process in connection with the solvent polarity. Studies of fluorescent dyes with solvatochromism are considered to be important, and solvatochromic luminogens can be used to evaluate solvent parameters. On the other hand, fluorescent organic molecules that are responsive to mechanical stimulus have attracted substantial interest because of their promising applications in mechanosensors and fluorescent switches (Chen et al., 2015; Chen et al., 2017; Chen et al., 2018; Chen et al., 2019; Wang et al., 2020; Zhang et al., 2020; Hu et al., 2021; Hu et al., 2021; Yin et al., 2021). In this work, we reported a TPE-modified rhodanine derivative (**Chart 1**), and the compound exhibited AIEE and mechanofluorochromic characteristics. Furthermore, this fluorescent molecule could selectively and sensitively detect Hg^{2+} in an acetonitrile solution and on test paper strips. Rhodanine-3-acetic acid is an electron acceptor, and the combination of the acceptor and TPE core

CHART 1 | The molecular structure of TPE-modified rhodanine derivative 1.



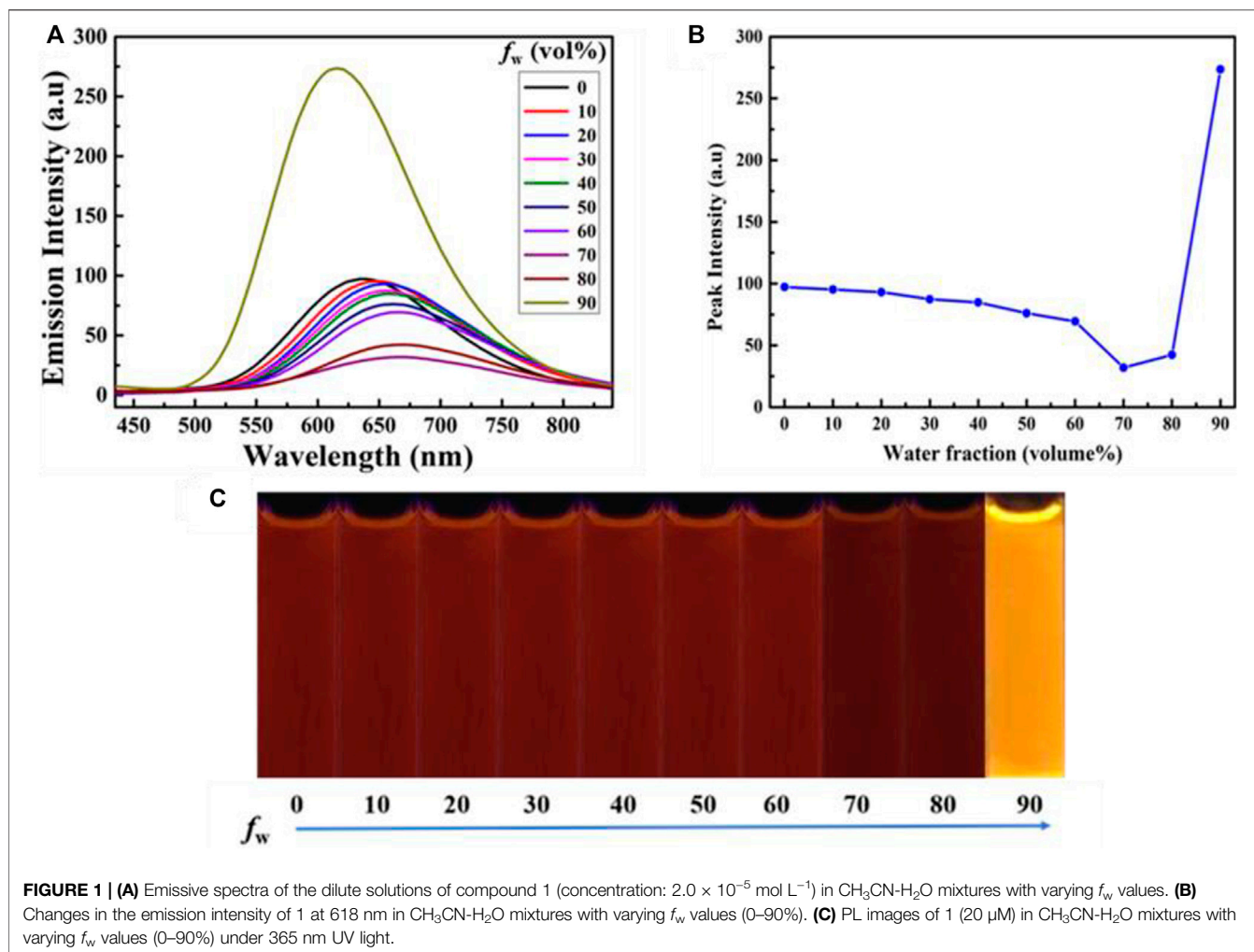


FIGURE 1 | (A) Emissive spectra of the dilute solutions of compound 1 (concentration: 2.0×10^{-5} mol L⁻¹) in CH₃CN-H₂O mixtures with varying f_w values. **(B)** Changes in the emission intensity of 1 at 618 nm in CH₃CN-H₂O mixtures with varying f_w values (0–90%). **(C)** PL images of 1 (20 μ M) in CH₃CN-H₂O mixtures with varying f_w values (0–90%) under 365 nm UV light.

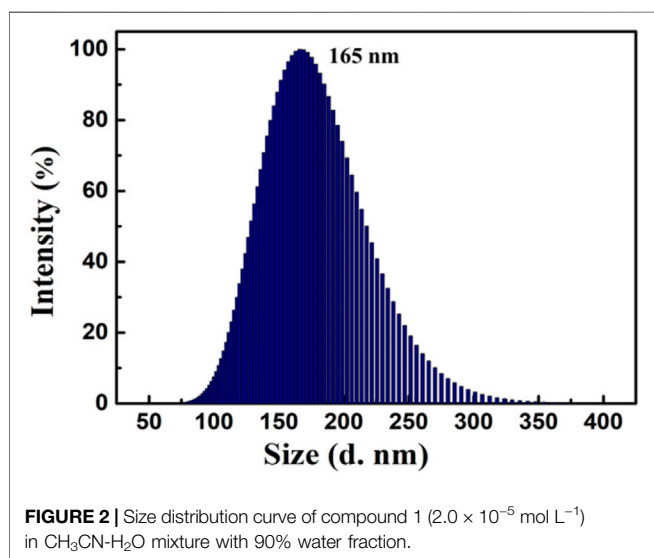
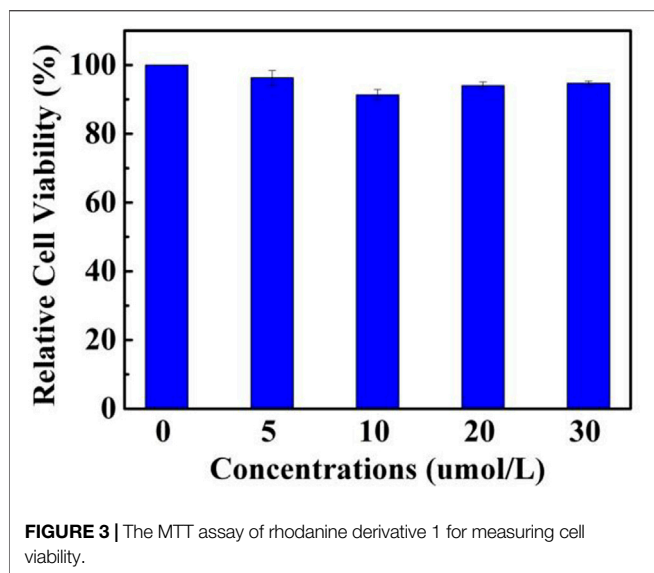


FIGURE 2 | Size distribution curve of compound 1 (2.0×10^{-5} mol L⁻¹) in CH₃CN-H₂O mixture with 90% water fraction.

provides a pull-push feature to the obtained target molecule. As a result, luminogen 1 also showed solvatochromic fluorescence behavior.

EXPERIMENTAL SECTION

General methods: This target compound 1 was synthesized according to the route shown in **Scheme 1**. All synthetic experiments were performed under dry argon atmosphere applying standard Schlenk techniques. 2-(4-Oxo-2-thioxothiazolidin-3-yl)acetic acid and other starting materials and reagents were purchased from Innochem (Beijing, China) and used without further purification. Compound I-1 was synthesized according to the reported literature (Zhao et al., 2012). In addition, ¹H NMR and ¹³C NMR spectra were collected on Bruker AVANCE NEO 500 MHz FT-NMR Spectrometer (500 MHz), chemical shift of internal standard tetramethylsilane at 0.00 ppm. Mass spectrum was collected by an ion trap MSD spectrometer (Agilent). Elemental analyses (C, H, N) were carried out with a PE CHN 2400 analyzer. Ultraviolet/Visible absorption spectra were measured on an Agilent 8453 UV-Vis spectrophotometer. Emission spectra were recorded on a Hitachi-F-4600 fluorescence spectrophotometer or an Edinburgh FLS1000 fluorescence spectrometer. DLS datum was recorded by NanoBrook 90Plus (Brookhaven Instruments). Fluorescence images were collected on an Olympus FV1000



confocal laser scanning microscope. Powder XRD experiments were carried out by Shimadzu XRD-6000 diffractometer with Ni-filtered and graphite-monochromated Cu K α radiation ($\lambda = 1.54 \text{ \AA}$, 40 kV, 30 mA).

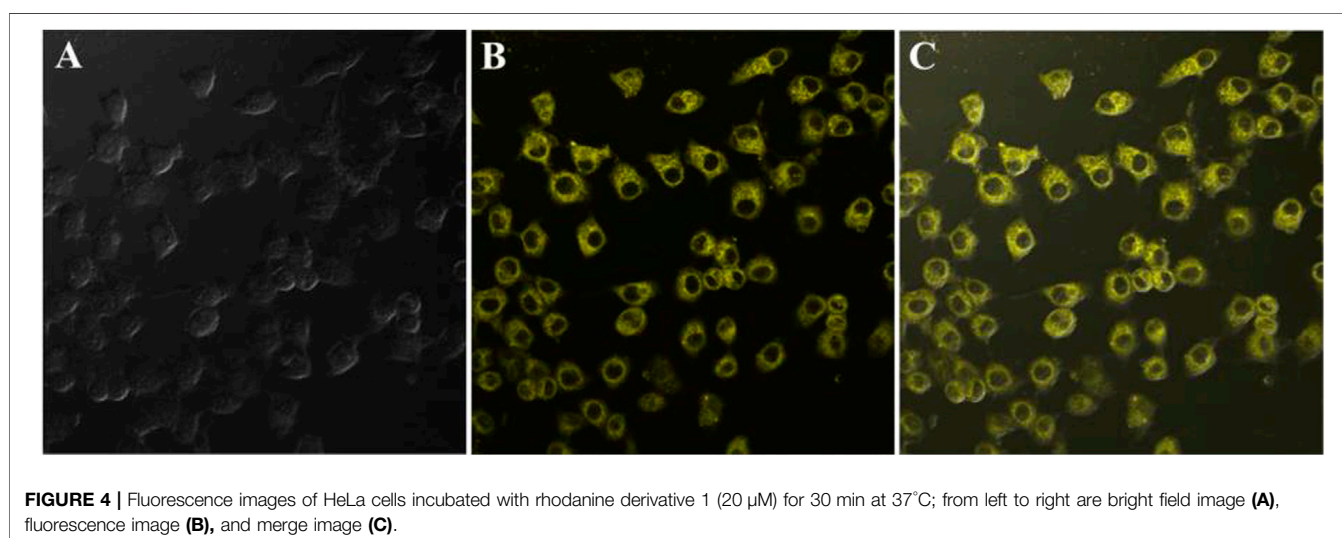
Synthesis of compound 1: A 100 ml two-necked round-bottom flask was evacuated under vacuum and then flushed with dry argon three times. Subsequently, compound I-1 (720.92 mg, 2.0 mmol), 2-(4-Oxo-2-thioxothiazolidin-3-yl) acetic acid (2.0 mmol), NH $_4$ OAc (2.0 mmol), and methanol (60 ml) were added into the round-bottom flask. After that, the mixture was refluxed for 24 h and then cooled to room temperature. After the disappearance of the starting materials, monitored by TLC board, the resulting mixture was extracted with dichloromethane and water, and then washed with brine three times. Organic layer was dried by anhydrous MgSO $_4$, then the organic solvent was removed under vacuum, the residues were purified by column chromatography on silica gel, affording

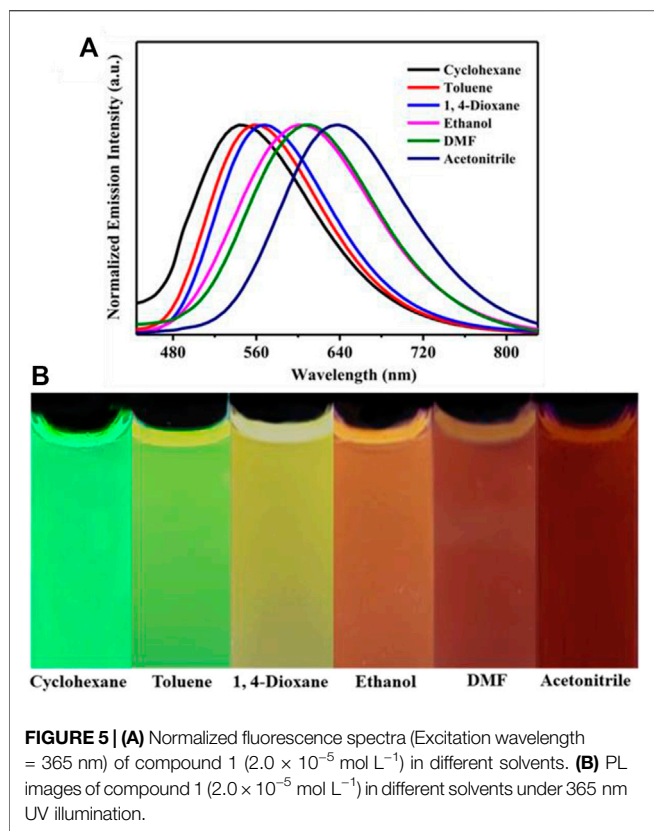
the corresponding target product 1 (yellow solid) in a yield of 62.6%. 1: $^1\text{H NMR}$ (500 MHz, DMSO- d_6): δ (ppm) = 13.48 (s, 1H), 7.79 (s, 1H), 7.46 (d, $J = 5 \text{ Hz}$, 2H), 7.18–7.13 (m, 11H), 7.02–6.97 (m, 6H), 4.73 (s, 2H). $^{13}\text{C NMR}$ (125 MHz, DMSO- d_6): δ (ppm) = 193.2, 167.4, 166.5, 146.5, 142.9, 142.8, 142.7, 142.3, 139.7, 133.5, 131.9, 131.0, 130.9, 130.8, 130.7, 130.6, 128.2, 128.0, 127.1, 127.0, 121.5, 45.1. HRMS (m/z): 533.1113 [M] $^+$ (calcd 533.1119). Anal. Calcd. For C $_{32}$ H $_{23}$ NO $_3$ S $_2$: C, 72.02; H, 4.34; N, 2.62. Found: C, 72.15; H, 4.25; N, 2.67.

RESULTS AND DISCUSSION

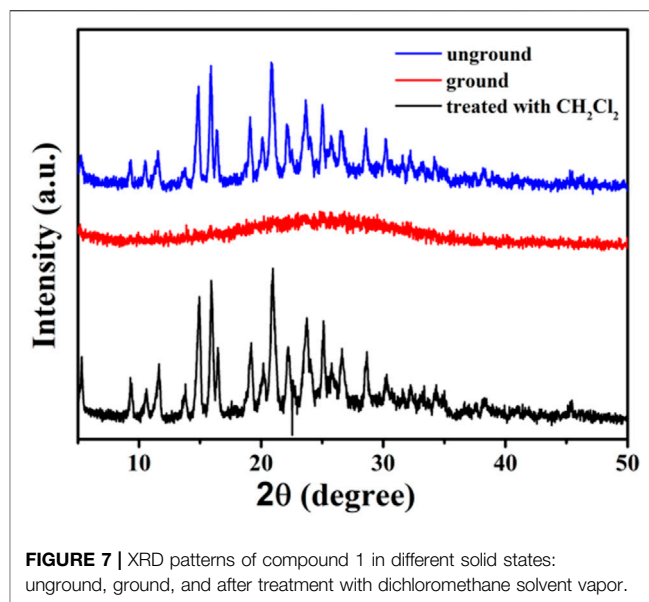
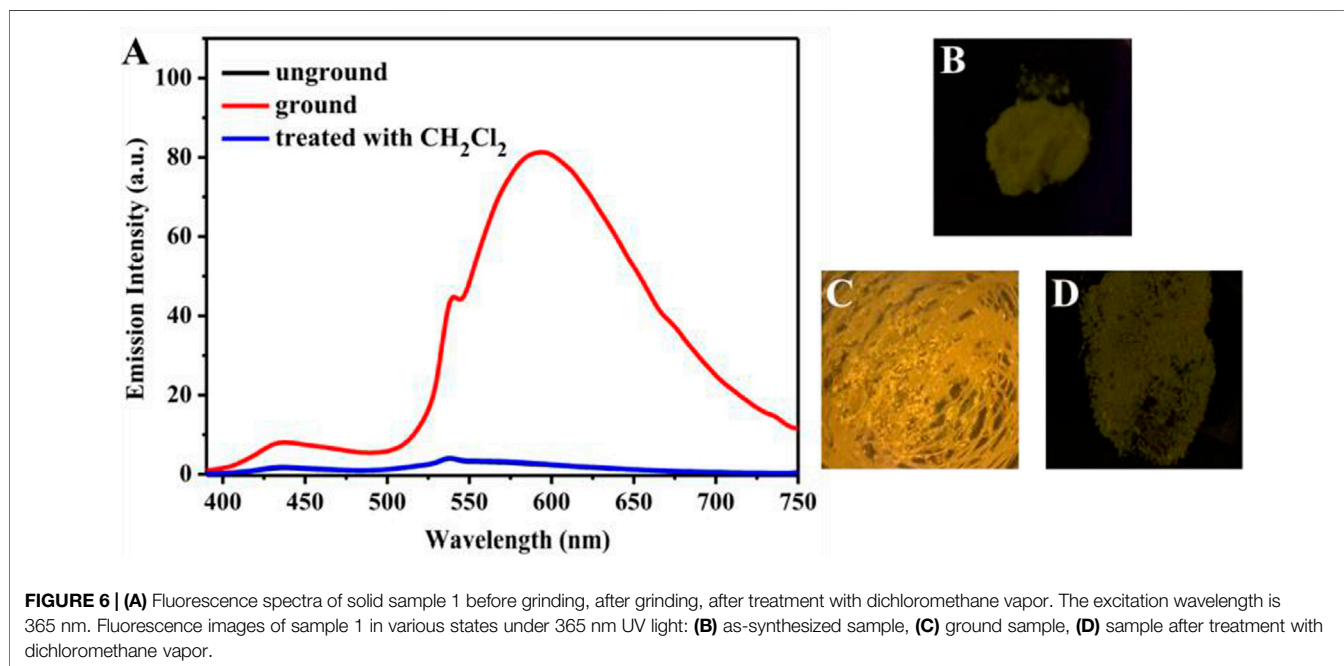
In order to investigate the aggregative-state emissive behavior of compound 1, the UV-Vis absorption spectra of compound 1 (20 μM) in CH $_3$ CN-H $_2$ O mixtures with different water fractions were initially measured. Obviously, level-off tails were noticed in the long-wavelength region as the water content increased (**Supplementary Figure S1**). Such a phenomenon indicated the formation of nano-aggregates (Leung et al., 2013). Next, the photoluminescence (PL) spectra of luminogenic molecule 1 (20 μM) in CH $_3$ CN-H $_2$ O mixtures with various volume fractions of water (f_w) were studied. As presented in **Figure 1**, luminogen 1 (20 μM) in pure CH $_3$ CN displayed weak red fluorescence due to an intramolecular charge transfer (ICT) from the TPE unit to the rhodanine-3-acetic acid unit, the fluorescence quantum yield of luminogen 1 (20 μM) in pure CH $_3$ CN was 0.7%, and the emission intensity of red fluorescence gradually weakened when the f_w value was continuously increased to 70%, which was attributed to the twisted ICT effect (Shen et al., 2012; Liu et al., 2019). When the f_w value was 90%, the quantum yield of luminogen 1 in the CH $_3$ CN-H $_2$ O mixture was 6.6%.

Interestingly, when the water content reached 90%, a bright orange fluorescence was observed. Water is a non-solvent for luminogen 1, increasing the f_w value in the mixed solvent leading to the transition of the compound from a well-dispersed state in pure CH $_3$ CN to aggregated particles in CH $_3$ CN-H $_2$ O mixture with 90% water





fraction. Indeed, the nano-aggregates obtained were confirmed by carrying out dynamic light scattering (DLS) experiment (Figure 2). The strong orange fluorescence of luminogen 1 was thus triggered by aggregation, and compound 1 exhibited typical AIEE feature.



In consideration of the remarkable AIEE nature of compound 1, the prepared fluorescent molecule was applied for cell imaging. HeLa cells were chosen as testing cells to culture and stain with luminogen 1, and the cell imaging effect was evaluated by a confocal laser scanning microscopy (CLSM). The standard MTT experiment suggested that the TPE-modified rhodanine derivative displayed low cytotoxicity (Figure 3). Subsequently, HeLa cells were incubated with AIEE-active compound 1 (20 μM) for 30 min at 37°C and the fluorescence images were collected by CLSM. As demonstrated in Figure 4, an intense yellow fluorescence was

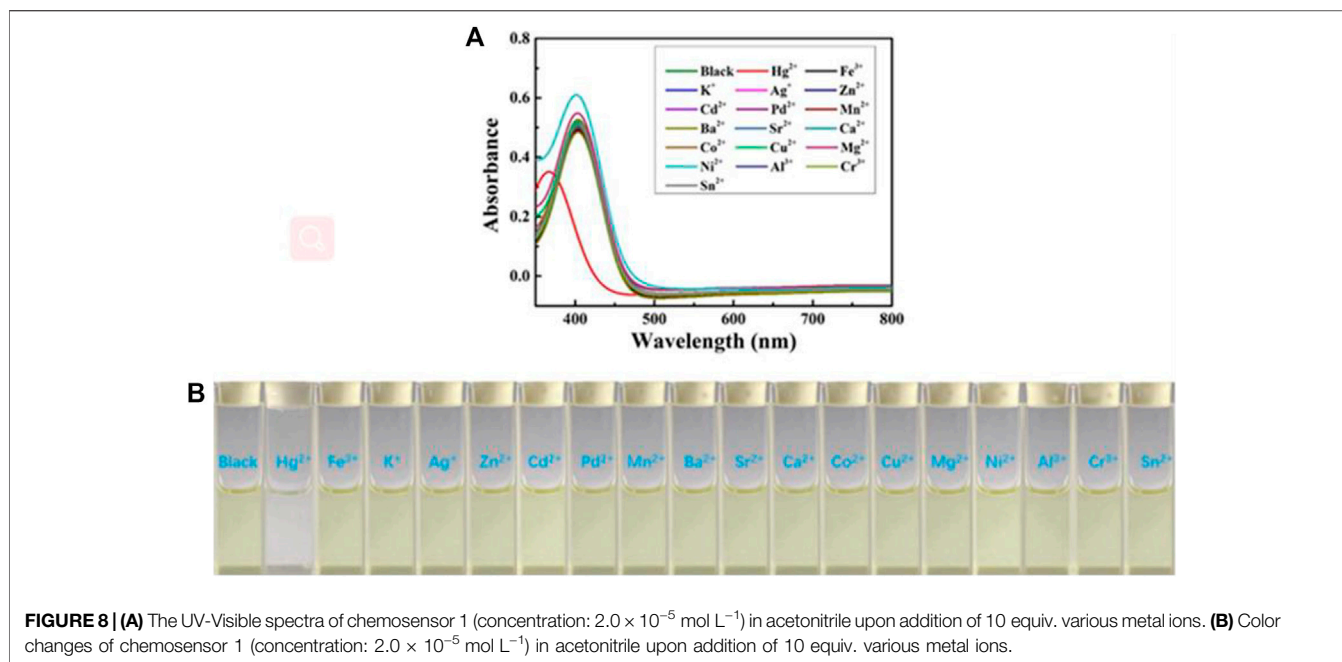


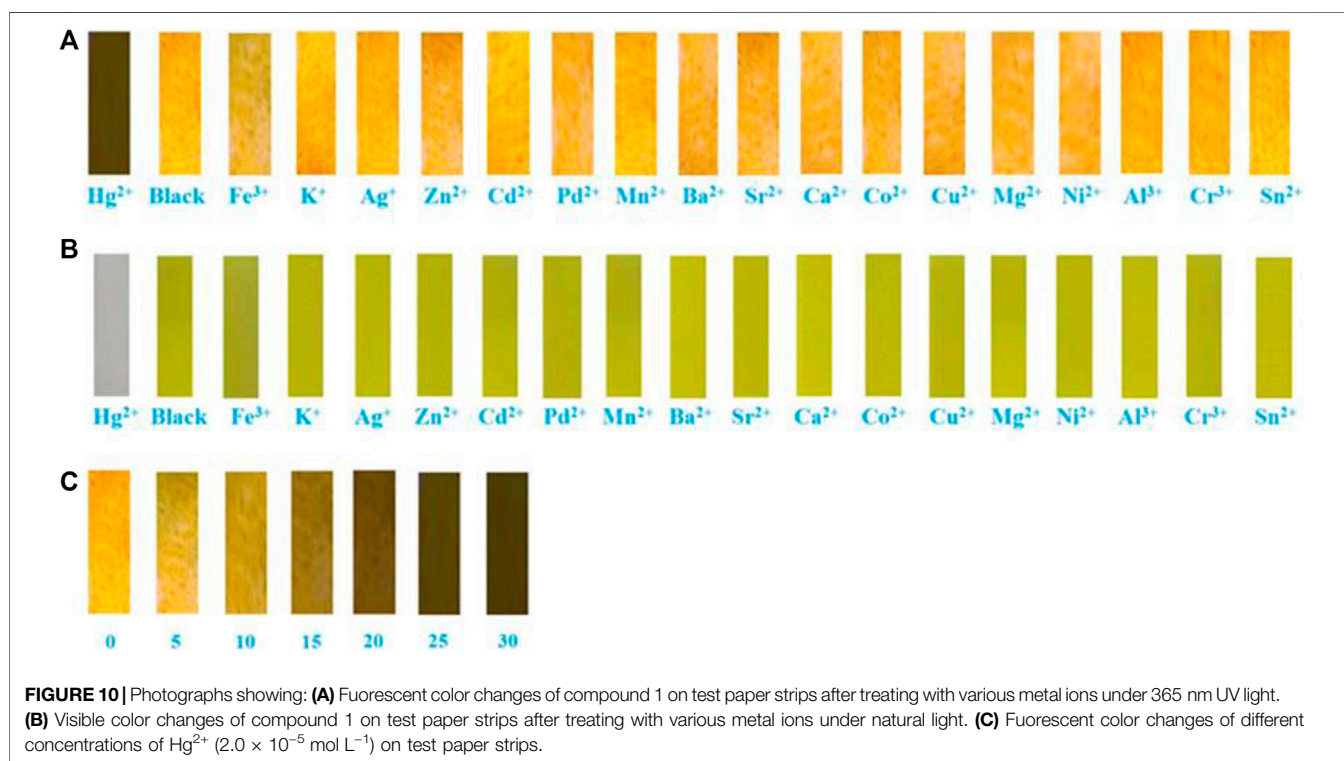
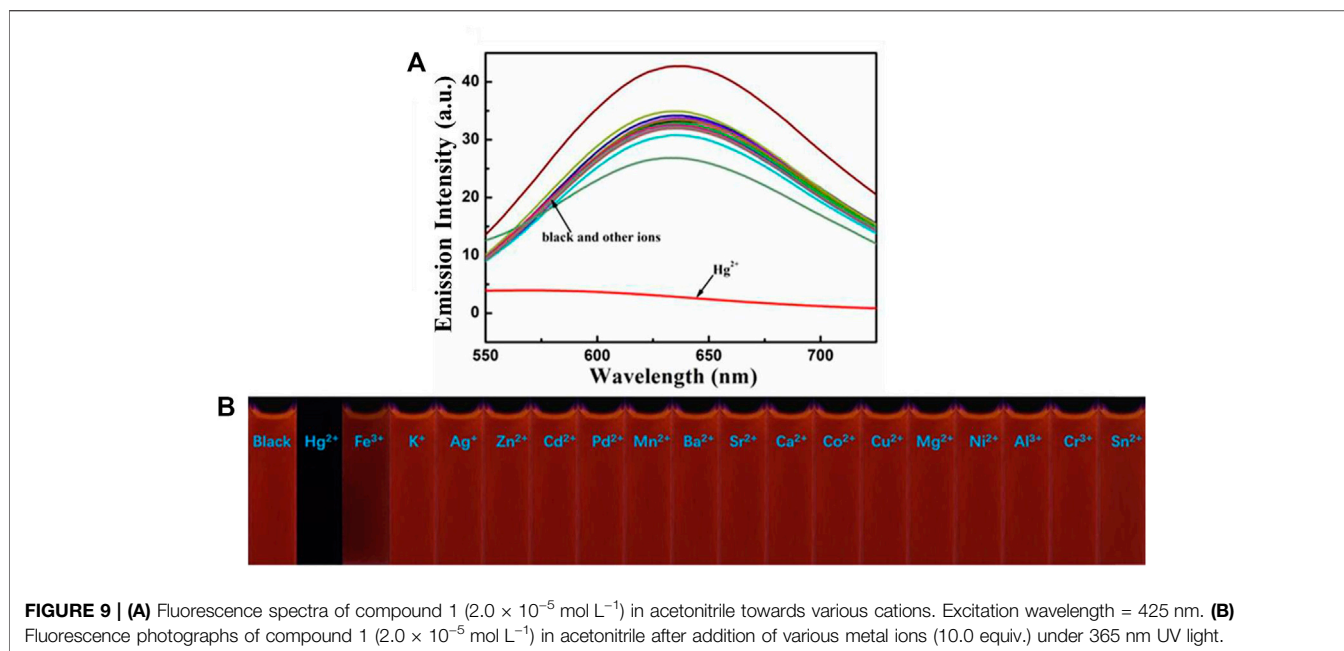
FIGURE 8 | (A) The UV-Visible spectra of chemosensor 1 (concentration: $2.0 \times 10^{-5} \text{ mol L}^{-1}$) in acetonitrile upon addition of 10 equiv. various metal ions. **(B)** Color changes of chemosensor 1 (concentration: $2.0 \times 10^{-5} \text{ mol L}^{-1}$) in acetonitrile upon addition of 10 equiv. various metal ions.

observed inside the cells. In addition, picture C, which is the overlap of pictures A and B, indicated that rhodanine derivative 1 possessed good cell imaging effect.

Introduction of electron acceptor rhodanine-3-acetic acid group to a TPE group may endue the target compound with not only the ICT effect but also with the solvatochromic behavior. As shown in **Figure 5**, luminogen 1 ($20 \mu\text{M}$) displayed various fluorescent colors, including green, yellow-green, yellow, orange, and red, in a series of solvents with increasing polarities (Cyclohexane < Toluene < 1,4-Dioxane < Ethanol < DMF < Acetonitrile). A striking red shift of the emission peak from 535 to 640 nm was recorded with the increasing solvent polarities. And polarity may be the dominant reason for the large red shift (Shen et al., 2012). We mainly studied the solvent polarity and the red shift of the emission peak, so we completed a uniform treatment of the intensity of the largest emission peak in different solvents, which was convenient and straightforward for this study. In a word, these results indicated that the fluorescence behavior of luminogen 1 was sensitive to solvent polarity, exhibiting strong solvatochromism phenomenon. In addition, as can be seen in **Figure 6**, the pristine solid sample 1 emitted weak yellow fluorescence. However, upon grinding, an obvious orange emission band with a λ_{max} at 594 nm was observed, and a bright orange fluorescence could be seen. When the orange-emitting sample was fumed with dichloromethane vapor for 30 s, the fluorescent color rapidly changed back to faint yellow. Therefore, luminogen 1 also exhibited reversible mechanochromic fluorescence feature.

By analyzing the obtained powder X-ray diffraction (PXRD) patterns of compound 1 before and after grinding (**Figure 7**), it was discovered that the fluorescent change from weak yellow emission to strong orange emission was attributed to crystalline-to-amorphous morphological transformation.

The colorimetric sensing ability of compound 1 toward Hg^{2+} was evaluated using UV-Vis absorption spectroscopy. Changes in the UV-Vis absorption spectra of 1 ($20 \mu\text{M}$) in acetonitrile upon addition of Hg^{2+} were shown in **Supplementary Figure S2**. After the concentration of Hg^{2+} was increased to 6 eq., a new absorption band with a maximum at 365 nm was observed. At the same time, the visible color of the solution changed from pale yellow to colourless. The fluorescence response of 1 to Hg^{2+} was illustrated in **Supplementary Figure S3**. Obviously, the fluorescence intensity of 1 gradually decreased as the Hg^{2+} concentration progressively increased from 0 to 10.0 equivalents, and the emissive color was transformed from red to colorless, and then followed by a plateau via further titration (**Supplementary Figure S4**). Based on the titration experiments, we calculated the detection limit of TPE-modified rhodanine derivative 1 for Hg^{2+} , which was $6.0 \times 10^{-7} \text{ mol L}^{-1}$ (**Supplementary Figure S5**). This quenching constant of 1 with Hg^{2+} was calculated to be $9.74 \times 10^4 \text{ M}^{-1}$ (**Supplementary Figure S6**). Furthermore, the Job's plot also demonstrated 1:1 stoichiometric ratio between 1 and Hg^{2+} (**Supplementary Figure S7**). Moreover, the binding interaction of compound 1 and Hg^{2+} was surveyed by ^1H NMR in dimethyl sulfoxide- d_6 . Apparently, 1 exhibited a singlet at 13.48 ppm of the carboxyl hydrogen (COOH) (**Supplementary Figure S8**), and the singlet at 13.48 ppm disappeared with new peaks at 4.3 and 7.8 ppm appeared when the analyte concentration was 10 equiv. We speculated that the carbonyl group on the rhodanine structure and the hydroxyl group of the carboxylic acid were combined with Hg^{2+} , which destroyed the original p conjugation and most of the π electron density would be transferred to the carbonyl carbon, thus causing a corresponding shift in the mass spectrum (Thamaraiselvi



et al., 2019). Furthermore, the binding interaction of compound 1 and Hg^{2+} (Hg^{2+} solution prepared with DMSO) was surveyed by ^1H NMR in dimethyl sulfoxide- d_6 again (**Supplementary Figure S8B**). On the basis of Pearson's Hard-Soft Acid-Base Theory (Ralph 1993), Hg^{2+} can interact preferentially with sulfur, oxygen, and nitrogen.

Besides, to further assess the binding mode of 1 toward Hg^{2+} , the probe was used to detect its molecular mass with 10.0 equiv. Hg^{2+} , the exact value at $m/z = 833.2428$ showed high affinity for Hg^{2+} combine $[1 + \text{H}^+ + \text{Hg}^{2+} + \text{NO}_3^- + \text{Cl}^-]^+$, which indicated the binding of 1 with Hg^{2+} with 1 : 1 stoichiometry (**Supplementary Figure S9**).

Next, the sensing capabilities of compound 1 were examined in acetonitrile through the addition of various cations, including Hg^{2+} , Fe^{3+} , K^+ , Ag^+ , Zn^{2+} , Cd^{2+} , Pd^{2+} , Mn^{2+} , Ba^{2+} , Sr^{2+} , Ca^{2+} , Co^{2+} , Cu^{2+} , Mg^{2+} , Ni^{2+} , Al^{3+} , Cr^{3+} , and Sn^{2+} . As demonstrated by **Figure 8**, when 10.0 equivalents of metal ions listed above were added to the solution, only Hg^{2+} caused a color change from pale yellow to colourless. The UV-Vis absorption spectrum of the diluted acetonitrile solution containing compound 1 with mercury ion showed a clear blue-shifted absorption peak at 365 nm, and the absorption peaks of the solution with other metal ions and blank probes were all at 410 nm. It can be shown that the selective recognition of compound 1 and mercury ion can be realized in the UV-Vis absorption spectra. Presumably, it was attributed to the structural changes caused by the selective complexation of fluorescent probe 1 with mercury ion. Meanwhile, as showed in **Figure 9**, the red fluorescence was quenched by the addition of Hg^{2+} (10.0 equiv.). Before and after addition of mercury ion, the fluorescence quantum efficiency of compound 1 ($2.0 \times 10^{-5} \text{ mol L}^{-1}$) in acetonitrile were 0.7 and 0.2%, respectively. The fluorescence spectrum of the dilute solution of acetonitrile containing compound 1 showed that the intensity of the emission peak at 625 nm was significantly reduced after adding 10 equivalents of mercury ion. However, when other metal cations were added separately into the solution containing compound 1, no notable fluorescent changes could be seen. It was inferred that the fluorescence probe 1 was complexed with mercury ion, which caused the structure of the fluorescence probe 1 to change, thus showing the effect of fluorescence “on-off.” This showed that the fluorescent probe 1 had excellent specific selectivity to mercury ion. Furthermore, as presented in **Supplementary Figure S10**, no remarkable interference was noticed when Hg^{2+} (10.0 equiv.) was added with other ions (10.0 equiv.).

Finally, the test strips were made for the detection of Hg^{2+} . Specifically, we added test strips with the same size to the acetonitrile solutions of chemosensor 1 containing different metal ions. After 15 s, they were taken out from the solutions and then dried in air naturally. Obviously, **Figure 10B** shows that the test strip containing 1 and Hg^{2+} hardly emitted fluorescence under 365 nm UV light, while the test strips containing 1 and other metal ions exhibited orange fluorescence, which was consistent with that of the blank test strip. Similarly, the test strip containing 1 and Hg^{2+} was almost colorless under natural light (**Figure 10B**), and the blank test strip and test strips containing 1 and other metal ions were yellow under natural light. Furthermore, as can be seen in **Figure 10C**, the fluorescent color of the test strip gradually changed from orange to colourless with the concentration of Hg^{2+} raising from 0 to $30 \times 10^{-5} \text{ mol L}^{-1}$. In order to study the effect of pH on compound 1, we tested the fluorescence characteristics of compound 1 in the range of pH (2–13). As depicted in **Supplementary Figure S13B**, the fluorescence intensity of compound 1 at 649 nm was relatively stable in the range of pH 3–7. With the increase of pH, the

fluorescence intensity of the blank probe gradually decreased, which was caused by the influence of the carboxylic acid on the rhodanine structure under alkaline conditions. The experimental results showed that compound 1 could be tested under acidic and neutral conditions.

CONCLUSION

In summary, a TPE-modified rhodanine derivative 1 was reported, and the compound with ICT effect exhibited typical AIEE and good cell imaging properties. Interestingly, the luminogenic molecule not only displayed solvatochromic fluorescence behavior but also displayed reversible mechanochromic fluorescence phenomenon. In addition, luminogen 1 could selectively and sensitively detect Hg^{2+} in an acetonitrile solution. Meanwhile, luminogen 1 could also be applied to detect Hg^{2+} on test paper strips. This work provides a valuable reference to the preparation of TPE-based multifunctional luminophors.

DATA AVAILABILITY STATEMENT

The original contributions presented in the study are included in the article/**Supplementary Material**, further inquiries can be directed to the corresponding authors.

AUTHOR CONTRIBUTIONS

ZC designed the project. ZC, J-JT, and D-DD wrote the manuscript. ZC, J-JT, D-DD, and LW performed the synthesis of compound 1. ZC, J-JT, D-DD, and LW conducted the characterization of compound 1. ZC and SP provided critical advice during the manuscript writing. All authors have given approval to the final version of the manuscript.

FUNDING

This study was financially supported by the National Natural Science Foundation of China (nos. 22061018, 21702079 and 41867053), the Natural Science Foundation for Distinguished Young Scholars of Jiangxi Province (20212ACB213003), and the Academic and Technical Leader Plan of Jiangxi Provincial Main Disciplines (20212BCJ23004).

SUPPLEMENTARY MATERIAL

The Supplementary Material for this article can be found online at: <https://www.frontiersin.org/articles/10.3389/fchem.2021.811294/full#supplementary-material>

REFERENCES

- An, B.-K., Kwon, S.-K., Jung, S.-D., and Park, S. Y. (2002). Enhanced Emission and its Switching in Fluorescent Organic Nanoparticles. *J. Am. Chem. Soc.* 124 (48), 14410–14415. doi:10.1021/ja0269082
- Bhalla, V., Tejpal, R., and Kumar, M. (2010). Rhodamine Appended Terphenyl: A Reversible "Off-On" Fluorescent Chemosensor for Mercury Ions. *Sensors Actuators B: Chem.* 151 (1), 180–185. doi:10.1016/j.snb.2010.09.024
- Chen, Z., Liu, G., Pu, S., and Liu, S. H. (2017). Carbazole-based Aggregation-Induced Emission (AIE)-active Gold(I) Complex: Persistent Room-Temperature Phosphorescence, Reversible Mechanochromism and Vapochromism Characteristics. *Dyes Pigm.* 143, 409–415. doi:10.1016/j.dyepig.2017.05.003
- Chen, Z., Liu, G., Pu, S., and Liu, S. H. (2018). Triphenylamine, Carbazole or Tetraphenylethylene-Based Gold(I) Complexes: Tunable Solid-State Room-Temperature Phosphorescence and Various Mechanochromic Luminescence Characteristics. *Dyes Pigm.* 159, 499–505. doi:10.1016/j.dyepig.2018.07.016
- Chen, Z., Nie, Y., and Liu, S. H. (2016). Fluorene-based Mononuclear Gold(I) Complexes: the Effect of Alkyl Chain, Aggregation-Induced Emission (AIE) and Mechanochromism Characteristics. *RSC Adv.* 6 (77), 73933–73938. doi:10.1039/c6ra17806e
- Chen, Z., Tang, J.-H., Chen, W., Xu, Y., Wang, H., Zhang, Z., et al. (2019). Temperature- and Mechanical-Force-Responsive Self-Assembled Rhomboidal Metallacycle. *Organometallics* 38 (21), 4244–4249. doi:10.1021/acs.organomet.9b00544
- Chen, Z., Zhang, J., Song, M., Yin, J., Yu, G.-A., and Liu, S. H. (2015). A Novel Fluorene-Based Aggregation-Induced Emission (AIE)-active Gold(I) Complex with Crystallization-Induced Emission Enhancement (CIEE) and Reversible Mechanochromism Characteristics. *Chem. Commun.* 51 (2), 326–329. doi:10.1039/c4cc08087d
- Cheng, S., Chen, Z., Yin, Y., Sun, Y., and Liu, S. (2021). Progress in Mechanochromic Luminescence of Gold(I) Complexes. *Chin. Chem. Lett.* doi:10.1016/j.ccllet.2021.05.049
- Dong, Y. Q., Lam, J. W. Y., and Tang, B. Z. (2015). Mechanochromic Luminescence of Aggregation-Induced Emission Luminogens. *J. Phys. Chem. Lett.* 6 (17), 3429–3436. doi:10.1021/acs.jpcltt.5b01090
- Feng, W., Xia, Q., Zhou, H., Ni, Y., Wang, L., Jing, S., et al. (2017). A Fluorescent Probe Based upon Anthracene-Dopamine Thioether for Imaging Hg²⁺ Ions in Living Cells. *Talanta* 167, 681–687. doi:10.1016/j.talanta.2017.03.012
- Gupta, R. C., Razi, S. S., Ali, R., Dwivedi, S. K., Srivastava, P., Singh, P., et al. (2017). An Efficient Hg²⁺ Ensemble Based on a Triazole Bridged Anthracene and Quinoline System for Selective Detection of Cyanide through Fluorescence Turn-Off-On Response in Solution and Live Cell. *Sensors Actuators B: Chem.* 251, 729–738. doi:10.1016/j.snb.2017.04.096
- Hu, H., Chen, Z., and Pu, S. (2021a). Fluorene-Based Aggregation-Induced Emission (AIE)-Active Tetraphenylethene Derivatives: The Effect of Alkyl Chain Length on Mechanofluorochromic Behaviors. *Tetrahedron Lett.* 67, 152846. doi:10.1016/j.tetlet.2021.152846
- Hu, J., Liu, Y., Zhang, X., Han, H., Li, Z., and Han, T. (2021b). Fabricating a Mechanochromic AIE Luminogen into a Wearable Sensor for Volatile Organic Compound (VOC) Detection. *Dyes Pigm.* 192, 109393. doi:10.1016/j.dyepig.2021.109393
- Huang, J., Sun, N., Chen, P., Tang, R., Li, Q., Ma, D., et al. (2014). Largely Blue-Shifted Emission through Minor Structural Modifications: Molecular Design, Synthesis, Aggregation-Induced Emission and Deep-Blue OLED Application. *Chem. Commun.* 50 (17), 2136–2138. doi:10.1039/c3cc49313j
- Kiani, M., Bagherzadeh, M., Meghdadi, S., Rabiee, N., Abbasi, A., Schenk-Joß, K., et al. (2020). Development of a Novel Carboxamide-Based Off-On Switch Fluorescence Sensor: Hg²⁺, Zn²⁺ and Cd²⁺. *New J. Chem.* 44 (27), 11841–11852. doi:10.1039/d0nj02595j
- Leung, C. W. T., Hong, Y., Chen, S., Zhao, E., Lam, J. W. Y., and Tang, B. Z. (2013). A Photostable AIE Luminogen for Specific Mitochondrial Imaging and Tracking. *J. Am. Chem. Soc.* 135 (1), 62–65. doi:10.1021/ja310324q
- Li, J., Ding, G., Niu, Y., Wu, L., Feng, H., and He, W. (2018). The Structural Properties of 5-Methyl-2-Phenyl-2 H -1,2,3-triazole-4- Carboxylic Acid and Chromogenic Mechanism on its Rhodamine B Derivatives to Hg²⁺ Ions. *Spectrochimica Acta A: Mol. Biomol. Spectrosc.* 200, 127–135. doi:10.1016/j.saa.2018.04.009
- Li, Z., Gao, X., Hu, X., Zhang, X., Jia, C., Liu, C., et al. (2021). Dithienylethenes Functionalized by Triphenylethene and Difluoroboron β -diketonate Fragments: Synthesis, Optical Switching Behavior and Fluorescent Turn-On Sensing for Volatile Organic Amines. *Dyes Pigm.* 192, 109422. doi:10.1016/j.dyepig.2021.109422
- Liu, Z., Jiang, Z., Yan, M., and Wang, X. (2019). Recent Progress of BODIPY Dyes with Aggregation-Induced Emission. *Front. Chem.* 7, 712. doi:10.3389/fchem.2019.00712
- Luo, J., Xie, Z., Lam, J. W. Y., Cheng, L., Tang, B. Z., Chen, H., et al. (2001). Aggregation-Induced Emission of 1-Methyl-1,2,3,4,5-Pentaphenylsilole. *Chem. Commun.* (18), 1740–1741. doi:10.1039/b105159h
- Ma, X., Chi, W., Han, X., Wang, C., Liu, S., Liu, X., et al. (2021). Aggregation-Induced Emission or Aggregation-Caused Quenching? Impact of Covalent Bridge between Tetraphenylethene and Naphthalimide. *Chin. Chem. Lett.* 32 (5), 1790–1794. doi:10.1016/j.ccllet.2020.12.031
- Mei, J., Leung, N. L. C., Kwok, R. T. K., Lam, J. W. Y., and Tang, B. Z. (2015). Aggregation-Induced Emission: Together We Shine, United We Soar!. *Chem. Rev.* 115 (21), 11718–11940. doi:10.1021/acs.chemrev.5b00263
- Nan, X., Huyan, Y., Li, H., Sun, S., and Xu, Y. (2021). Reaction-based Fluorescent Probes for Hg²⁺, Cu²⁺ and Fe³⁺/Fe²⁺. *Coord. Chem. Rev.* 426, 213580. doi:10.1016/j.ccr.2020.213580
- Pearson, R. G. (1993). The Principle of Maximum Hardness. *Acc. Chem. Res.* 26 (5), 250–255. doi:10.1021/ar00029a004
- Que, E. L., Domaille, D. W., and Chang, C. J. (2008). Metals in Neurobiology: Probing Their Chemistry and Biology with Molecular Imaging. *Chem. Rev.* 108 (5), 1517–1549. doi:10.1021/cr078203u
- Shen, X. Y., Yuan, W. Z., Liu, Y., Zhao, Q., Lu, P., Ma, Y., et al. (2012). Fumaronitrile-Based Fluorogen: Red to Near-Infrared Fluorescence, Aggregation-Induced Emission, Solvatochromism, and Twisted Intramolecular Charge Transfer. *J. Phys. Chem. C* 116 (19), 10541–10547. doi:10.1021/jp303100a
- Singh, P., Kumar, K., Kaur, N., Kaur, S., and Kaur, S. (2020). Perylene Diimide Dye Threaded with Dual-React Able Sites for Detection of H₂S and Hg²⁺: Diagnostic Kit and Cell Imaging. *Dyes Pigm.* 180, 108448. doi:10.1016/j.dyepig.2020.108448
- Song, Z., Kwok, R. T. K., Ding, D., Nie, H., Lam, J. W. Y., Liu, B., et al. (2016). An AIE-Active Fluorescence Turn-On Bioprobe Mediated by Hydrogen-Bonding Interaction for Highly Sensitive Detection of Hydrogen Peroxide and Glucose. *Chem. Commun.* 52 (65), 10076–10079. doi:10.1039/c6cc05049b
- Tan, K.-Y., Li, C.-Y., Li, Y.-F., Fei, J., Yang, B., Fu, Y.-J., et al. (2017). Real-Time Monitoring ATP in Mitochondrion of Living Cells: A Specific Fluorescent Probe for ATP by Dual Recognition Sites. *Anal. Chem.* 89 (3), 1749–1756. doi:10.1021/acs.analchem.6b04020
- Tang, A., Yin, Y., Chen, Z., Fan, C., Liu, G., and Pu, S. (2019). A Multifunctional Aggregation-Induced Emission (AIE)-active Fluorescent Chemosensor for Detection of Zn²⁺ and Hg²⁺. *Tetrahedron* 75 (36), 130489. doi:10.1016/j.tet.2019.130489
- Thamaraiselvi, P., Duraipandy, N., Kiran, M. S., and Easwaramoorthi, S. (2019). Triarylamine Rhodamine Derivatives as Red Emissive Sensor for Discriminative Detection of Ag⁺ and Hg²⁺ Ions in Buffer-free Aqueous Solutions. *ACS Sustainable Chem. Eng.* 7, 9865–9874. doi:10.1021/acssuschemeng.9b00417
- Tian, M., Wang, C., Ma, Q., Bai, Y., Sun, J., and Ding, C. (2020). A Highly Selective Fluorescent Probe for Hg²⁺ Based on a 1,8-Naphthalimide Derivative. *ACS Omega* 5 (29), 18176–18184. doi:10.1021/acsomega.0c01790
- Tong, J., Wang, Y., Mei, J., Wang, J., Qin, A., Sun, J. Z., et al. (2014). A 1,3-Indandione-Functionalized Tetraphenylethene: Aggregation-Induced Emission, Solvatochromism, Mechanochromism, and Potential Application as a Multiresponsive Fluorescent Probe. *Chem. Eur. J.* 20 (16), 4661–4670. doi:10.1002/chem.201304174
- Wang, X.-Y., Yin, Y., Yin, J., Chen, Z., and Liu, S. H. (2021). Persistent Room-Temperature Phosphorescence or High-Contrast Phosphorescent Mechanochromism: Polymorphism-dependent Different Emission Characteristics from a Single Gold(I) Complex. *Dalton Trans.* 50 (22), 7744–7749. doi:10.1039/d1dt00959a
- Wang, Z., Li, H., Peng, Z., Wang, Z., Wang, Y., and Lu, P. (2020). Preparation and Photophysical Properties of Quinazoline-Based Fluorophores. *RSC Adv.* 10 (51), 30297–30303. doi:10.1039/d0ra05701k
- Xu, T.-Y., Nie, H.-J., Li, J.-M., and Shi, Z.-F. (2020). Highly Selective Sensing of Fe³⁺/Hg²⁺ and Proton Conduction Using Two Fluorescent Zn(ii) Coordination Polymers. *Dalton Trans.* 49 (32), 11129–11141. doi:10.1039/d0dt02327b

- Yang, X., Qin, X., Li, Y., Yan, M., Cui, Y., and Sun, G. (2018). TBET-based Ratiometric Fluorescent Probe for Hg²⁺ with Large Pseudo-stokes Shift and Emission Shift in Aqueous media and Intracellular Colorimetric Imaging in Live HeLa Cells. *Biosens. Bioelectron.* 121, 62–71. doi:10.1016/j.bios.2018.09.004
- Yang, Y., Yin, C., Huo, F., Chao, J., and Zhang, Y. (2014). Highly Selective Relay Recognition of Hydrogen Sulfide and Hg(II) by a Commercially Available Fluorescent Chemosensor and its Application in Bioimaging. *Sensors Actuators B: Chem.* 204, 402–406. doi:10.1016/j.snb.2014.07.108
- Yang, Z., Qin, W., Leung, N. L. C., Arseneault, M., Lam, J. W. Y., Liang, G., et al. (2016). A Mechanistic Study of AIE Processes of TPE Luminogens: Intramolecular Rotation vs. Configurational Isomerization. *J. Mater. Chem. C* 4 (1), 99–107. doi:10.1039/c5tc02924d
- Yin, W., Yang, Z., Zhang, S., Yang, Y., Zhao, L., Li, Z., et al. (2021b). A Positively Charged Aggregation-Induced Emission (AIE) Luminogen as an Ultra-sensitive Mechanochromic Luminescent Material: Design, Synthesis and Versatile Applications. *Mater. Chem. Front.* 5 (6), 2849–2859. doi:10.1039/d0qm01047b
- Yin, Y., Chen, Z., Li, R.-H., Yuan, C., Shao, T.-Y., Wang, K., et al. (2021c). Ligand-Triggered Platinum(II) Metallocycle with Mechanochromic and Vapochromic Responses. *Inorg. Chem.* 60 (13), 9387–9393. doi:10.1021/acs.inorgchem.1c00233
- Yin, Y., Hu, H., Chen, Z., Liu, H., Fan, C., and Pu, S. (2021a). Tetraphenylethene or Triphenylethylene-Based Luminophors: Tunable Aggregation-Induced Emission (AIE), Solid-State Fluorescence and Mechanofluorochromic Characteristics. *Dyes Pigm.* 184, 108828. doi:10.1016/j.dyepig.2020.108828
- Zhang, J. F., Zhou, Y., Yoon, J., and Kim, J. S. (2011). Recent Progress in Fluorescent and Colorimetric Chemosensors for Detection of Precious Metal Ions (Silver, Gold and Platinum Ions). *Chem. Soc. Rev.* 40 (7), 3416–3429. doi:10.1039/c1cs15028f
- Zhang, M., Li, Y., Gao, K., Li, Z., Liu, Y., Liao, Y., et al. (2020). A Turn-On Mechanochromic Luminescent Material Serving as Pressure Sensor and Rewritable Optical Data Storage. *Dyes Pigm.* 173, 107928. doi:10.1016/j.dyepig.2019.107928
- Zhao, N., Yang, Z., Lam, J. W. Y., Sung, H. H. Y., Xie, N., Chen, S., et al. (2012). Benzothiazolium-Functionalized Tetraphenylethene: An AIE Luminogen with Tunable Solid-State Emission. *Chem. Commun.* 48 (69), 8637–8639. doi:10.1039/c2cc33780k
- Zheng, X., Zhu, W., Zhang, C., Zhang, Y., Zhong, C., Li, H., et al. (2019). Self-Assembly of a Highly Emissive Pure Organic Imine-Based Stack for Electroluminescence and Cell Imaging. *J. Am. Chem. Soc.* 141 (11), 4704–4710. doi:10.1021/jacs.8b13724

Conflict of Interest: The authors declare that the research was conducted in the absence of any commercial or financial relationships that could be construed as a potential conflict of interest.

Publisher's Note: All claims expressed in this article are solely those of the authors and do not necessarily represent those of their affiliated organizations, or those of the publisher, the editors, and the reviewers. Any product that may be evaluated in this article, or claim that may be made by its manufacturer, is not guaranteed or endorsed by the publisher.

Copyright © 2022 Tian, Deng, Wang, Chen and Pu. This is an open-access article distributed under the terms of the Creative Commons Attribution License (CC BY). The use, distribution or reproduction in other forums is permitted, provided the original author(s) and the copyright owner(s) are credited and that the original publication in this journal is cited, in accordance with accepted academic practice. No use, distribution or reproduction is permitted which does not comply with these terms.